Holzforschung, Vol. 63, pp. 340–347, 2009 • Copyright © by Walter de Gruyter • Berlin • New York. DOI 10.1515/HF.2009.061

Experimental and numerical determination of the hygroscopic warping of cross-laminated solid wood panels

Thomas Gereke[1,*], Per Johan Gustafsson[2], Kent Persson[2] and Peter Niemz[1]

[1] ETH Zurich, Institute for Building Materials (Wood Physics), Zurich, Switzerland

[2] Lund University, Division of Structural Mechanics, Lund, Sweden

*Corresponding author.
ETH Zurich, Institute for Building Materials (Wood Physics), Schafmattstrasse 6, 8093 Zurich, Switzerland
E-mail: gereket@ethz.ch

Abstract

The moisture-induced warping of three-layered cross-laminated solid wood panels made of Norway spruce was studied. The panels were exposed to different climate conditions at 65% and 100% relative humidity at the two panel faces. The results showed increasing cup deformation with an increasing relative thickness of the outer layers. The annual growth ring orientation was found to have a significant influence on the magnitude of the cup deformation. Measurements and numerical simulations of the moisture distribution within the panel were made in order to provide data for numerical simulations of the warping. A distinctive moisture profile with a conspicuous influence of the adhesive bond lines was found. The coefficient of diffusion of the adhesive bond lines was determined from the measurements and simulations. The mechanical material model used for the warping simulations takes into account elastic strain, moisture-induced swelling, and mechano-sorptive strain. The simulations showed good agreement with the warping test results. The most important material parameters for the cup deformation, which were identified in a parametric study of a panel with vertically oriented annual rings, are the moduli of elasticity and the swelling coefficients in the longitudinal and radial direction. Furthermore, the mechano-sorptive coefficient in radial direction was found to have a significant influence on warp.

Keywords: adhesive joint; cross-lamination; cup; moisture; panel; spruce (*Picea abies*); warp.

Introduction

This work focuses on moisture-induced deformations in three-layered cross-laminated solid wood panels with a symmetrical build-up, where the fiber direction of the middle layer is oriented perpendicular to that of the outer layers. Dimensional stability, i.e., the ability of resistance to warp, is of main interest in the application of wood panels. The cross-lamination of the layers establishes advantages to avoid warp. The moisture-induced expansion/contraction of each single layer is partly restrained by the adjacent layers. The free swelling and shrinkage of adjacent layers differ circa by a factor of 10 (radial/longitudinal) to 20 (tangential/longitudinal). As a consequence of this difference, stresses and even cracks may occur. Warping was observed in large-scale panels. This reduces the serviceability in the practice. Considerable distortions (warp) in the form of cup and twist may occur due to a climate gradient (Figure 1). The cup deformation may occur in the *xz*- and the *yz*-plane. This is often termed cup and bow deformation, respectively (Ormarsson 1999).

Miscellaneous research concerning cross-laminated wood panels has been carried out in recent years. Mainly mechanical properties have been tested (Donzé et al. 2003; Tobisch 2006; Czaderski et al. 2007). Design recommendations have been developed (Blass and Görlacher 2003; Jöbstl and Schickhofer 2007) and elastic parameters have been determined by eigenfrequency measurements (Gülzow et al. 2008). Moisture and heat transport properties, such as diffusion resistance, equilibrium moisture content, and thermal conductivity, have been studied as well (Popper et al. 2004a,b; Bader et al. 2007). Tobisch (2006) tested the dimensional stability of cross-laminated panels exposed to a moisture gradient in a double climate chamber. The results showed an increase in warping with an increasing relative thickness of the outer layers. Gereke et al. (2008) studied the warping in a climate difference and the moisture-induced stresses due to a single climate step in cross-laminated panels made of beech wood and heat-treated beech wood. The knowledge about the moisture behavior of cross-laminated panels is, however, still limited.

To model the hygroscopic distortions – e.g., by means of a finite element simulation – the moisture distribution in the panel is needed. Moisture transport in wood below the fiber saturation point is a process governed by diffusion, which may be simulated by Fick's law (Siau 1995). The material parameter needed is the diffusion coefficient D [m s^{-2}]. It is well documented in the literature for Norway spruce (Vanek and Teischinger 1989; Siau 1995; Hukka 1999). Information about the moisture diffusion coefficient of adhesives is, on the other hand, very limited. In this study, the diffusion coefficient of the adhesive was determined by a combination of experimental measurements and numerical simulations of the moisture distribution in the panels.

Water diffuses into wood through a boundary layer that provides resistance to the diffusion if airflow at the wood surface is slow. The flux vector $\boldsymbol{J}$ perpendicular to the surface with the normal vector $\boldsymbol{n}$ is driven by the difference in concentration of the wood surface $c_{surface}$ and the concentration c_{air} that corresponds to the relative humidity (RH) of the ambient air:

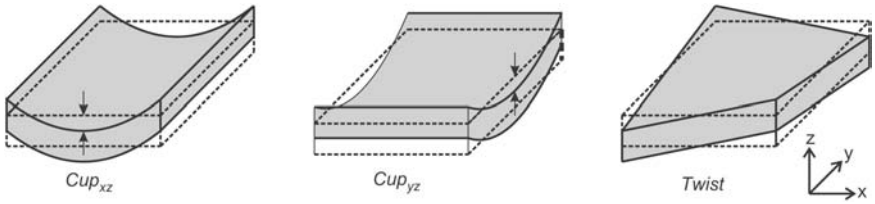

Figure 1 The types of warp deformation.

$$\mathbf{nJ} = h(c_{air} - c_{surface}), \tag{1}$$

where h [m s^{-1}] symbolizes a mass transfer coefficient. Diffusion is expressed in terms of concentration of water relative to the dry volume of wood. Thus, the effect of swelling is omitted from the mass balance.

The mechanical material model

$$\dot{\boldsymbol{\varepsilon}} = \dot{\boldsymbol{\varepsilon}}_{el} + \dot{\boldsymbol{\varepsilon}}_{\omega} + \dot{\boldsymbol{\varepsilon}}_{\omega\sigma} = (\mathbf{S}\dot{\boldsymbol{\sigma}} + \dot{\mathbf{S}}\boldsymbol{\sigma}) + \boldsymbol{\alpha}\dot{\omega} + \mathbf{m}\boldsymbol{\sigma}\dot{\omega} \tag{2}$$

was validated on distortions of sawn timber by Ormarsson (1999). The total strain rate is the sum of elastic strain rate $\dot{\boldsymbol{\varepsilon}}_{el}$, moisture-induced swelling $\dot{\boldsymbol{\varepsilon}}_{\omega}$, and mechano-sorptive deformation $\dot{\boldsymbol{\varepsilon}}_{\omega\sigma}$, where a dot denotes the derivative with respect to time. Creep strains are neglected from the material formulation. The elastic compliance matrix **S** containing the moisture dependent moduli of elasticity E, shear moduli G, and Poisson's ratios ν (Bodig and Jayne 1993). Thus, the rate of the compliance matrix $\dot{\mathbf{S}}$ has to be considered. The vector α containing either the shrinkage or the swelling coefficients in the orthotropic directions. The mechano-sorptive strain rate follows an expression proposed by Takemura (1967) and Leicester (1971). The mechano-sorptive property matrix is defined as (Ranta-Maunus 1990; Santaoja et al. 1991; Ormarsson 1999):

$$\mathbf{m} = \begin{bmatrix} m_L & -\mu_{RL}m_R & -\mu_{TL}m_T & 0 & 0 & 0 \\ -\mu_{LR}m_L & m_R & -\mu_{TR}m_T & 0 & 0 & 0 \\ -\mu_{LT}m_L & -\mu_{RT}m_R & m_T & 0 & 0 & 0 \\ 0 & 0 & 0 & m_{LR} & 0 & 0 \\ 0 & 0 & 0 & 0 & m_{LT} & 0 \\ 0 & 0 & 0 & 0 & 0 & m_{RT} \end{bmatrix}. \tag{3}$$

Material and methods

Moisture measurements

The test setup was made according to the standard DIN EN ISO 12572 (2001). Cylindrical specimens corresponding to panel type AR90 (Table 1) were exemplarily investigated, measuring 30 mm in thickness and 140 mm in diameter. They were initially conditioned at 20°C and 65% RH. The specimens were fastened with rubber sleeves on cups, which were filled with distilled water. The sleeves prevented the specimens from moisture sorption at the edges. A climate difference of 20°C and 65/100% RH was applied by placing the cups in a climate room. After 14, 21, 28, and 170 days, two rectangular samples with a dimension of 40 mm×80 mm were cut from the center of each specimen. Subsequently, they were split into layers of 5 mm thickness, and moisture content (MC) was determined by drying.

Warp measurements

In Table 1, the thicknesses and growth ring orientations of the panels and the individual layers are presented. The panels were made of Norway spruce (*Picea abies* [L.] Karst.) and glued either in a laboratory with one-component polyurethane (adhesive application 200 g m^{-2}, one-sided, forming pressure 0.8 MPa, pressing time 3 h) or glued by an industrial manufacturer with urea resin. Both the edges of the boards and the layer-to-layer surfaces were glued. The material was conditioned at 20°C and 65% RH until equilibrium was reached before and after the gluing.

The group of specimens indicated by the abbreviation AR relates to experiments where the influence of the annual growth ring orientation, θ, as defined in Figure 2, was studied. Three orientations were tested: 0°, 45°, and 90°. The group of specimens indicated by LR relates to testing where the influence of the layer ratio (LR) on cup deformation was studied. LR is defined by

$$\mathrm{LR} = \frac{2a_{OL}}{a_{tot}}, \tag{4}$$

where $2a_{OL}$ is the thickness of the two outer layers and a_{tot} is the panel thickness. LR was varied from 0.37 to 0.67.

Table 1 Panel characteristics.

Group	ID	Production[1]	a_{BL}=a_{TL} (mm)[2]	a_{ML} (mm)[2]	a_{tot} (mm)[2]	θ (°)	LR (-)
Annual	AR0	A	10	10	30	0	0.67
growth ring	AR45	A	10	10	30	45	0.67
orientation	AR90	A	10	10	30	90	0.67
Layer	LR37	B	7	24	38	90	0.37
ratio	LR52	B	7	13	27	90	0.52
	LR57	A	10	15	35	90	0.57

[1]A – laboratory, 1C polyurethane, board width 100 mm; B – industry, urea resin, board width 26±1 mm.
[2]a – thickness, BL – bottom layer, TL – top layer, ML – middle layer, tot – total.

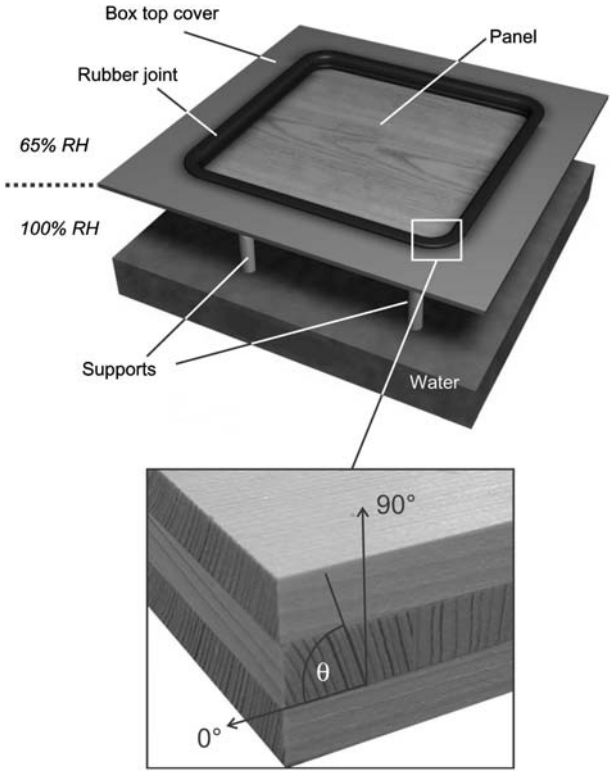

Figure 2 Test setup of the hygroscopic warping experiments and definition of annual ring angle θ.

The warping test method used was identical to that described by Gereke et al. (2008). The edges of the samples were sealed with lacquer to enforce the moisture flow within the panels in the thickness direction. The specimens were then placed in a box on three supports as illustrated in Figures 2 and 3. The contact area between the panel edges and the box top cover was insulated by a rubber joint. The climate difference of 65% RH and 100% RH was induced. These two levels of RH were obtained by means of water in the bottom of the box and a constantly conditioned climate room, in which the test setup was stored. Relative displacements in the *z*-direction of the measuring points, indicated in Figure 3, were recorded by means of dial gauges placed in a steel plate. Stop positions guaranteed identical placement of the steel plate in every measurement. The measurements of displacements were made for 31 days.

The cup deformation in the *xz*-plane (Figure 1) was determined as:

$$cup_{xz} = \frac{1}{2}(\bar{u}_z^{A,D,G} + \bar{u}_z^{C,F,J}) - \bar{u}_z^{B,E,H} \tag{5}$$

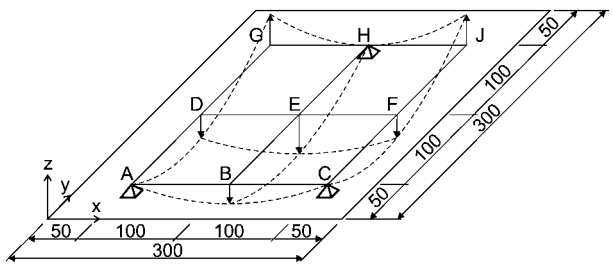

Figure 3 Dimensions in mm, location of measuring points, and coordinate system (*x*: fiber direction of the outer layers, *y*: fiber direction of the middle layer).

and the cup deformation in the *yz*-plane as:

$$cup_{yz} = \frac{1}{2}(\bar{u}_z^{A,B,C} + \bar{u}_z^{G,H,J}) - \bar{u}_z^{D,E,F.} \tag{6}$$

The notation $\bar{u}_z^{i,j,k}$ indicates the mean value of the displacements in the measuring points *i*, *j*, and *k* as shown in Figure 3. Twist deformation is omitted from the analysis, as it is small compared to cup deformation.

Material data

Moisture model

A one-dimensional diffusion model with a total of 340 eight-node volume elements along the thickness was applied (100 elements in each 10 mm thick wood layer and 20 elements in each 0.1 mm thick adhesive layer). The material parameter necessary for modeling diffusion according to Fick's law is the diffusion coefficient *D* [m² s⁻¹]. It was implemented into the material model by:

$$D_T(\omega) = 8.0 \cdot 10^{-11} e^{4\omega}, \qquad t \geq t^* \tag{7}$$

$$D_T^*(\omega, t) = D_T(\omega)\left[(1-\kappa)\frac{t}{t^*} + \kappa\right], \quad t < t^*. \tag{8}$$

The subscript *T* refers to diffusion in the transverse direction where identical properties in radial and tangential direction were assumed. Eq. (7) is an expression found by Toratti (1992), but the amount of dependency on MC was increased by Hanhijärvi (1995). The diffusion coefficient of wood strongly depends on the MC. With increasing MC the resistance to diffusion decreases and, thus, *D* increases. If $t < t^*$, the diffusion coefficient increases linearly from κD_T at the initial state ($t = 0$) to D_T at $t = t^*$ [Eq. (8)]. This reduction of D_T in the beginning of the analysis refers to the effect that water diffuses into wood as water vapor and is then absorbed by the cell walls. During this process, the diffusion rate is lower and the behavior is significant non-Fickian. It is thought that it is an unsteady state phenomenon related to sorption (Wadsö 1994). The reduction factor in Eq. (8) is $\kappa = 0.45$ [-] and the reduction time is $t^* = 1000$ h.

It is assumed that moisture diffuses through the adhesive as water vapor. According to Siau (1995) water vapor diffusion in wood slows down at higher MC. Thus, the following formulation was evaluated from the experimental tests:

$$D_{adh}(\omega) = C_1 \cdot \omega^{-C_2} + C_3 \tag{9}$$

The diffusion coefficient was determined by fitting the simulated curves to the experimental data. The shape factors are $C_1 = 9.17 \cdot 10^{-13}$ m² s⁻¹, $C_2 = 0.51$ [-] and $C_3 = -2.39 \cdot 10^{-12}$ m² s⁻¹.

The dependency of the concentration *c* on the relative humidity φ under isothermal conditions of $T = 20$°C

$$c(\varphi) = f_1\varphi^5 + f_2\varphi^4 + f_3\varphi^3 + f_4\varphi^2 + f_5\varphi + f_6 \tag{10}$$

has been found for spruce wood with $\rho_{0,wood} = 450$ kg m⁻³. The shape factors in Eq. (10) are $f_1 = 170.81$, $f_2 = -406.49$, $f_3 = 366.60$, $f_4 = -150.82$, $f_5 = 32.91$, and $f_6 = -1.09\ 10^{-3}$ (all non-dimensional). Consequently, the concentrations corresponding to the conditions in ambient air and the initial conditions are $c_{initial} = c_{air,top} = 5.60$ kg m⁻³ relating to $\varphi = 65\%$ and $c_{air,bottom} = 13.01$ kg m⁻³ relating to $\varphi = 100\%$ [Eq. (1)]. The mass

transfer coefficient h [m s^{-1}] of the boundary layer has been proposed by Hanhijärvi (1995) as:

$$h(\omega) = 3.2 \cdot 10^{-8}\, e^{4\omega}. \quad (11)$$

Mechanical model

Eight-node volume elements were used for the modeling. The fineness of the element mesh was chosen in order to obtain accurate results. The mesh density (number of elements):

$$NOE = N_x \cdot N_y \cdot (3N_z + 6) \quad (12)$$

was chosen as $N_x = 60$, $N_y = 120$, and $N_z = 5$, which are the number of elements in the global panel directions and the thickness mesh density of one wood layer (N_z). The adhesive layers were modeled by three volume elements in the thickness. The annual ring orientation was taken into account by rectangular local coordinate systems. Thus, a possible curvature of the annual rings and different lamellas within a layer were not considered.

The elastic parameters describing the compliance matrix **S**, Eq. (2), depend on the MC. From the findings of Neuhaus (1981) the following relation between the elastic parameters S (may be substituted by E, G or ν) and the MC could be found:

$$S = a_0 + a_1\omega + a_2\omega^2 + a_3\omega^3 \quad (13)$$

The shape factors a_k ($k = 0 \ldots 3$) are presented in Table 2. The data show that the moduli decrease with MC. E_T and E_R decrease within the hygroscopic range to approximately 50% of their value at the oven-dry state, while E_L only decreases to 85%. The shear moduli also decrease with MC: G_{LR} and G_{TL} decrease to approximately 50% and G_{RT} decreases to 30% from the oven-dry state to the fiber saturation point. The Poisson's ratio show a differing behavior: ν_{LR} remains nearly constant within the hygroscopic range, while ν_{TL} and ν_{TR} increase when the MC is increased.

The swelling coefficients were chosen according to Neuhaus (1981) and Sell (1997) to $\alpha_R = 1.7 \cdot 10^{-3}$ and $\alpha_T = 3.3 \cdot 10^{-3}$, and according to Dahlblom et al. (1999) (see also Ormarsson 1999) to $\alpha_L = 5.0 \cdot 10^{-5}$ (all non-dimensional).

The mechano-sorptive material parameters are based on results obtained by Santaoja et al. (1991) and Mårtensson (1992) and are set to be independent of the MC. The mechano-sorption coefficients in the orthotropic directions and planes that describe the mechano-sorption material matrix ***m*** [Eq. (3)] are $m_L = 1.0 \cdot 10^{-4}$, $m_R = 0.15$, $m_T = 0.2$, $m_{LR} = 8.0 \cdot 10^{-3}$, $m_{LT} = 8.0 \cdot 10^{-3}$, and $m_{RT} = 0.8$ (all MPa^{-1}). The coupling coefficients between the different directions are chosen as $\mu_{LR} = 0$, $\mu_{LT} = 0$, and $\mu_{RT} = 1$.

The adhesive, polyurethane, is assumed to act as a linear elastic isotropic material (Konnerth et al. 2007). The adhesive layers were assumed to be 0.1 mm thick. The elastic properties were chosen according to the tests of Konnerth et al. (2007) as $E_{adh} = 470$ MPa and $\nu_{adh} = 0.3$.

Table 2 Parameters a_k of the relation between the moduli of elasticity E, the shear moduli G, the Poisson's ratios ν, and moisture content [Eq. (13)] according to Neuhaus (1981), $0\% \leq \omega \leq 28\%$.

Parameter	a_0	a_1	a_2	a_3
E_L (MPa)	12 792	1522	-90 073	188 504
E_R (MPa)	1000	361	-20 917	46 665
E_T (MPa)	506	500	-13 499	29 733
G_{LR} (MPa)	763	593	-19 861	47 671
G_{LT} (MPa)	881	139	-13 925	27 691
G_{RT} (MPa)	61	-107	-617	1725
ν_{LR} (-)	0.046	0.136	-0.456	-0.214
ν_{LT} (-)	0.021	0.257	-1.435	2.190
ν_{RT} (-)	0.153	1.075	3.980	-19.1

Results and discussion

Moisture

The calculated moisture profiles and the measured MC are shown in Figure 4. The climate difference resulted in distinctive moisture profiles. The influence of the glue lines is obvious and very significant. The largest gradient in MC could be detected between the bottom and the middle layer. These two layers showed a rapid increase in moisture during the first 14 days and also a significant increase in moisture from day 14 to 170 (Figure 5). The MC in the top layer did not change very much from day 14 to day 170.

Deformations and stresses

The results of the experimental tests after 31 days are listed in Table 3. Major cupping was found in the *yz*-plane since the perpendicular to fiber direction of the outer layers is in the *y*-direction. This results in a dominant swelling of the bottom layer in this direction. Due to the

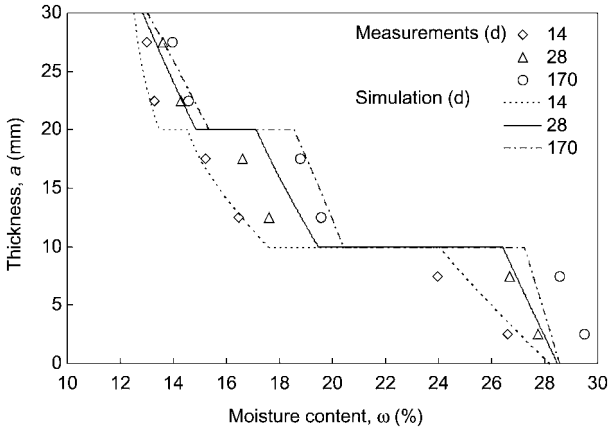

Figure 4 Measured and calculated moisture profiles.

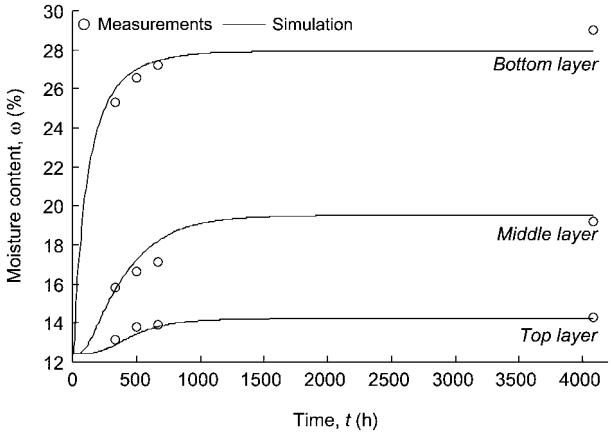

Figure 5 History plots of simulated moisture contents in the individual layers compared to the measurements. The studied material points of the simulations were located in the middle of each layer.

hindering by the middle layer, the panel warps in the *yz*-plane. The simulated warping of panel AR90 is displayed in Figure 6. The Figure shows that the edges moved upwards while the center moved downwards.

The influence of the annual growth ring orientation on the cup deformation is conspicuous (Table 3) and governed by the difference in swelling, stiffness properties, and material orientation. The largest cup was found for panels with horizontal annual rings (AR0) reflecting the large swelling of the bottom layer. Tangential swelling is approximately two times higher compared to radial swelling as it occurs in series AR90. The smallest cupping was recorded for the panels with $\theta = 45°$ (AR45), which most probably is due to the very small stiffness of softwood in that direction. It is approximately one-half of the tangential stiffness and approximately one-quarter of the radial stiffness as a result of the small G_{RT} (Keunecke et al. 2008).

The tests of different LRs show increased cupping cup_{yz} with increased LR (Table 3). The simulated results of a variation of $0.5 \leq LR \leq 0.8$ are plotted in Figure 7 for the panel thicknesses 20 mm and 30 mm. An increased LR yields an increased ratio of outer layers, i.e., a larger ratio of transverse oriented fibers in the *y*-direction. This effect leads to a larger cup_{yz} at higher LRs. The results show an exponential increase in cup deformation.

The experimentally obtained time variation of cup_{yz} is illustrated in Figure 8. Almost all panels attain their maximum cup between day 3 and day 12. Series AR45 and LR37 showed no significant maximum. For AR45 cup_{yz} became constant from day 5, whereas for LR37 a slightly

Table 3 Measured warping after 31 days.

ID	n	ρ_0 (kg m^{-3})	cup_{xz} (mm)	cup_{yz} (mm)
AR0	6	411	0.06 (0.05)	0.42 (0.05)
AR45	6	407	0.06 (0.06)	0.22 (0.08)
AR90	6	431	0.10 (0.15)	0.27 (0.08)
LR37	6	459	0.11 (0.19)	0.08 (0.02)
LR52	6	461	0.07 (0.09)	0.14 (0.04)
LR57	3	451	0.04 (0.27)	0.12 (0.08)

Data are mean and (standard deviation), ID according to Table 1. n – number of samples, ρ_0 – oven-dry density (dry mass/dry volume).

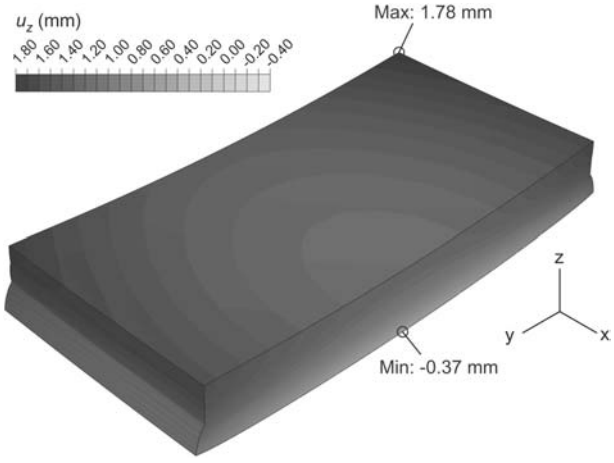

Figure 6 Simulated warp in a panel of series AR90 (one-half of the panel is displayed, displacements ×10, $t = 744$ h).

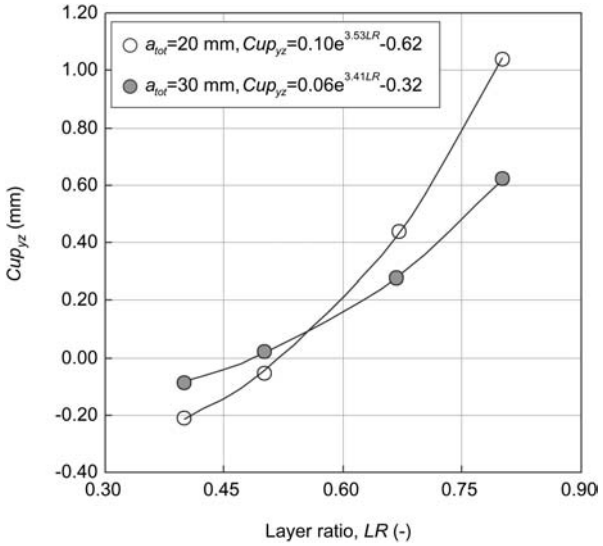

Figure 7 Simulated influence of the layer ratio LR on cup_{yz} for the panel thicknesses, 20 mm and 30 mm, $t = 744$ h.

increased cup_{yz} was recorded during the whole testing period. The MC of the bottom layer was found to increase rapidly (Figure 5). Hence, the expansion of the bottom layer, which is mainly in the *y*-direction, leads to a strong increase in cup_{yz}. The decrease in cup_{yz} after the maximum is reached is caused by an increase in MC of the middle layer and later of the top layer. The moisture increase and, therefore, swelling of these two layers act in opposition to the deformation of the bottom layer. Thus, cup_{yz} decreases and cup_{xz} increases. The simulated history plot of cupping in AR90 shows good agreement with the experimental test results (Figure 8).

Compared to beech panels, as investigated by Gereke et al. (2008), spruce panels showed good dimensional stability. The maximum cup_{yz} in three-layered cross-laminated beech panels with layer thicknesses of 10 mm and $LR = 0.67$ was detected at 1.14 mm. The cup in spruce panels was measured to be 70% smaller (AR90).

A sensitivity study of the mechanical material parameters was performed on panel type AR90. Almost no influence could be detected for varying the shear moduli and the Poisson's ratios. Panel type AR90 also acts

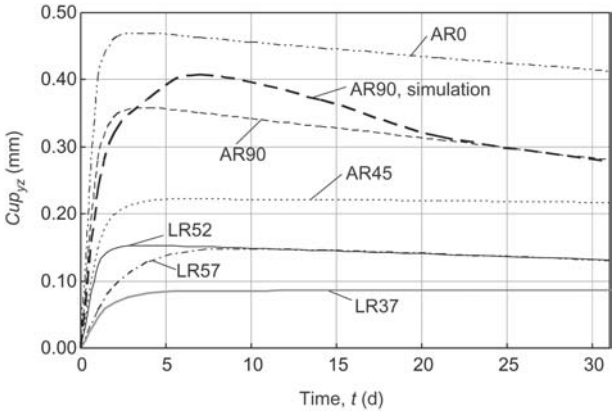

Figure 8 Non-linear regression of the time variation of the cup deformation in the *yz*-plane, cup_{yz}. For the denominations AR and LR, see Table 1 and the experimental section.

slightly sensitive on a modification of E_T. Figure 9 shows the influence of a 30% increase and a 30% decrease of E_L, E_R, α_L, α_R, m_L, and m_R in the individual layers and in the complete panel. The cupping cup_{yz} is significantly influenced by a change of the longitudinal parameters E_L and α_L in the middle layer and of the radial parameters E_R and α_R in the outer layers. The cup deformation cup_{xz} is significantly influenced only by a change of the parameters in the outer layers.

The mechano-sorptive strain was found to be very important for the cup deformation and for the results obtained in the parameter study. The mechano-sorptive coefficient m_R affects cup_{yz} with approximately 54% when decreased and -34% when increased. If omitting the mechano-sorptive effect, then the simulated cupping would become approximately 10 times higher and deviate very much from the cupping recorded in the experimental tests.

The mechano-sorptive strain is also important for the influence on the cupping of E_R and E_L. Increase of these two parameters, all other parameters kept constant, yielded decreased cupping if mechano-sorption is considered in the analysis and increased cupping if not considered. With an increase in the coefficients of hygroexpansion, the deformations increase and vice versa. A variation of α_L in the outer layers of 30% influences cup_{xz} by approximately 30%. In contrast, the variation of E_L, E_R, and α_R has almost no influence on cup_{xz} if the mechano-sorptive strain increment is considered. The modification of the coefficient of hygroexpansion causes a larger expansion of the layers in the appropriate direction. The longitudinal hygroexpansion influences the major direction. This results in a larger cup_{xz}, but only slightly changes cup_{yz}. The panel reveals the opposite behavior when α_R is modified. Here, the minor direction is mainly affected.

The stress distribution σ_y (radial direction) along the y-axis in the middle of the panel ($x = 150$ mm) is displayed for $z = 0$ mm (bottom face) and $z = 10$ mm (in the bottom layer at the glue line) in Figure 10. Stresses are significantly influenced by a variation of E_R and α_R, which lead to increased stresses. The variation of the mechano-

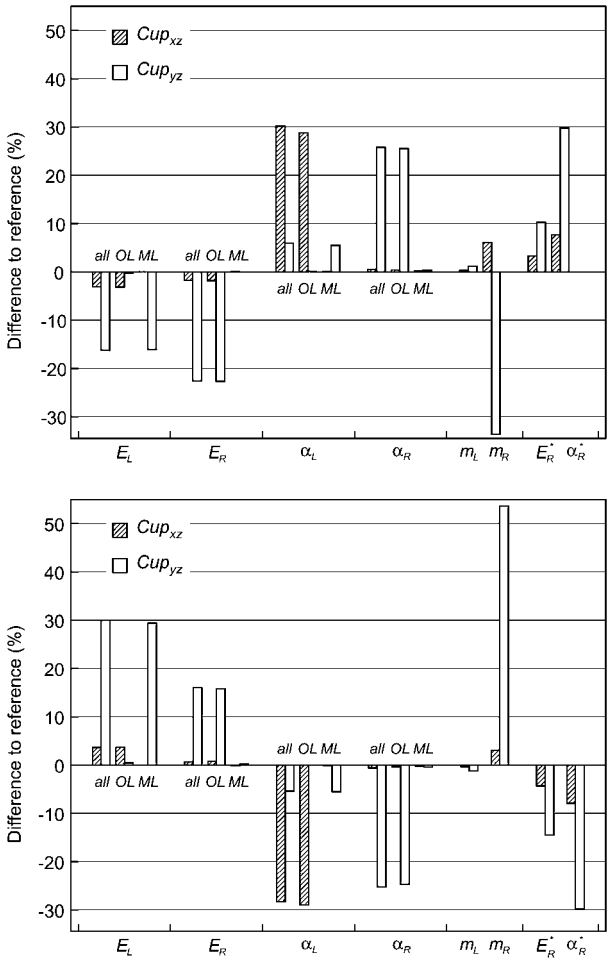

Figure 9 Relative change of the cup of panel type AR90 caused by 30% increase (upper) and 30% decrease (lower) of material parameter values for the complete panel (all) and the individual layers (OL, outer layer, ML, middle layer). *The mechano-sorptive fraction is omitted both in the parameter study and in the reference calculation.

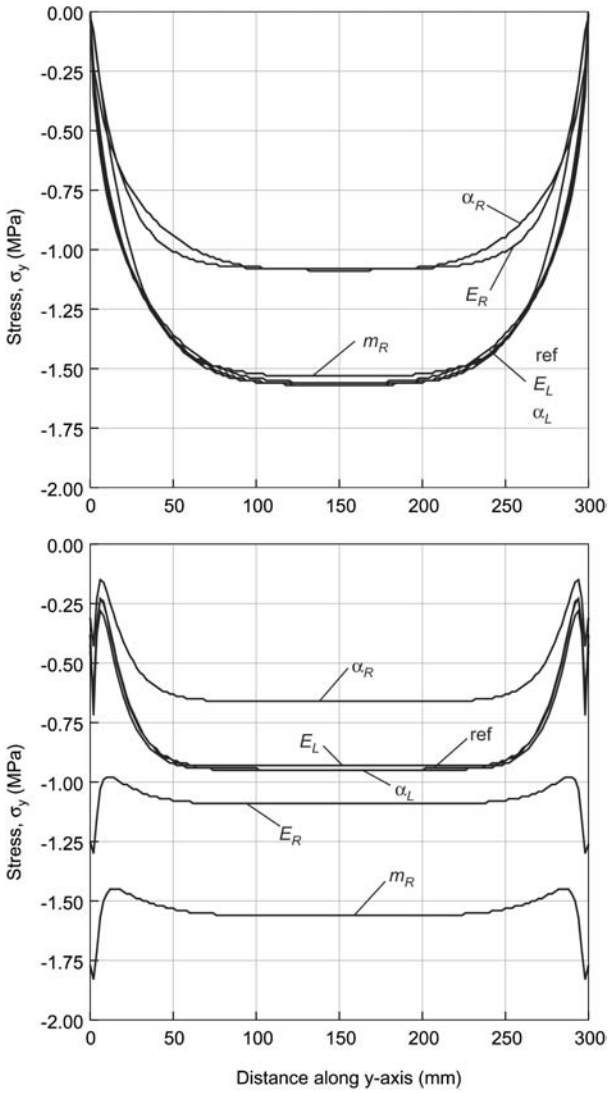

Figure 10 Simulated stress distribution σ_y along the y-axis in the bottom layer in panel AR90 after 744 h of climate difference 65/100% RH, $x = 150$ mm, $z = 0$ mm (upper), and $z = 10$ mm (lower), 30% decrease of the material parameter values; ref: reference panel.

sorptive coefficient m_R resulted in decreased stresses at the glue line.

The stiffness of the glue line influences the warping only in a slight manner. In a range up to $E_{adh}=10$ GPa, which conforms with results obtained by Konnerth et al. (2006, 2007), we observed a linear decrease in cup_{yz} of 5%, while cup_{xz} is not influenced. Thus, the influence on warping of potentially different moduli of elasticity of the two adhesives applied in the experimental tests can be neglected.

Conclusions

The hygroscopic warping of three-layered cross-laminated solid wood panels is mainly affected by the stiffness, the moisture-induced swelling, and the mechano-sorptive coefficient in the minor direction. These parameters can be altered by changing the layer ratio and the orientation of the annual growth rings. According to the results of this study, the orientation of the annual growth rings should be chosen as $\theta=45°$. The low stiffness perpendicular to the grain leads to small cuppings. Good results were obtained for $\theta=90°$ as well. The small moisture-induced swelling in the radial direction leads to small cuppings. $\theta=0°$ should be avoided in practical applications. Furthermore, the LR should be chosen as small as possible but without losing the barrier effect due to the cross-lamination. Depending on the panel thickness, the outer layers can become thin. Small thickness results in increased risk of cracking in the outer layers when the panel is exposed to drying. Therefore, moisture-induced stresses and cracking should be studied in future work. The possibilities and effects of alterations of the panel structure, e.g., by using some alternative middle layer material, should also be studied.

Acknowledgements

The authors gratefully acknowledge support from the European Cooperation in the Field of Scientific and Technical Research (COST Action E49).

References

Bader, H., Niemz, P., Sonderegger, W. (2007) Investigation on the influence of the panel composition on selected properties of three-layer solid wood panels. Holz Roh Werkst. 65:173–181.

Blass, H.J., Görlacher, R. (2003) Bemessung im Holzbau: Brettsperrholz – Berechnungsgrundlagen. Holzbau Kalender. 2:580–598.

Bodig, J., Jayne, B.A. Mechanics of Wood and Wood Composites. Krieger Publishing Company, Malabar, FL, 1993.

Czaderski, C., Steiger, R., Howald, M., Olia, S., Gülzow, A., Niemz, P. (2007) Tests and calculations on 3-layered cross-laminated solid wood panels supported at all edges. Holz Roh Werkst. 65:383–402.

Dahlblom, O., Persson, K., Petersson, H., Ormarsson, S. (1999) Investigation of variation of engineering properties of spruce. In: Proceedings of the 6th International IUFRO Wood Drying Conference: Wood Drying Research and Technology for Sustainable Forestry beyond 2000, Stellenbosch, South Africa. pp. 253–262.

DIN EN ISO 12572. (2001) Hygrothermal performance of building materials and products – Determination of water vapour transmission properties.

Donzé, M., Niemz, P., Hurst, A. (2003) Untersuchungen zu Eigenschaften mehrschichtiger Massivholzplatten. Wood Res. 48:27–36.

Gereke, T., Schnider, T., Hurst, A., Niemz, P. (2008) Identification of moisture-induced stresses in cross-laminated wood panels from beech wood (*Fagus sylvatica* L.). Wood Sci. Technol. Online first: DOI 10.1007/s00226-008-0218-1.

Gülzow, A., Gsell, D., Steiger, R. (2008) Non-destructive evaluation of elastic parameters of square-shaped cross-laminated solid wood panels, built up symmetrically with 3 layers. Holz Roh Werkst. 66:19–37.

Hanhijärvi, A. (1995) Modelling of creep deformation mechanisms in wood. PhD thesis, Technical Research Centre of Finland, Espoo, Finland.

Hukka, A. (1999) The effective diffusion coefficient and mass transfer coefficient of Nordic softwood as calculated from drying measurements. Holzforschung 53:534–540.

Jöbstl R.A., Schickhofer, G. (2007) Traglastnachweis für Brettsperrholz auf Basis der starren Verbundtheorie unter Berücksichtigung von Systemeffekten. In: Proceedings of the 39 Fortbildungskurs SAH "Praktische Anwendung von Massivholzplatten", Weinfelden, Switzerland. pp. 9–23.

Keunecke, D., Hering, S., Niemz, P. (2008) Three-dimensional elastic behaviour of common yew and Norway spruce. Wood Sci. Technol. 42:633–647.

Konnerth, J., Jäger, A., Eberhardsteiner, J., Müller, U., Gindl, W. (2006) Elastic properties of adhesive polymers. II. Polymer films and bond lines by means of nanoindentation. J. Appl. Polym. Sci. 102:1234–1239.

Konnerth, J., Gindl, W., Müller, U. (2007) Elastic properties of adhesive polymers. Part I: polymer films by means of electronic speckle pattern interferometry. J. Appl. Polym. Sci. 103:3936–3939.

Leicester, R.M. (1971) A rheological model for mechano-sorptive deflections of beams. Wood Sci. Technol. 5:211–220.

Mårtensson, A. (1992) Mechanical behaviour of wood exposed to humidity variations. PhD thesis, Lund University, Lund, Sweden.

Neuhaus, F.-H. (1981) Elastizitätszahlen von Fichtenholz in Abhängigkeit von der Holzfeuchtigkeit. PhD thesis, Ruhr-University Bochum, Germany.

Ormarsson, S. (1999) Numerical analysis of moisture-related distortions in sawn timber. PhD thesis, Chalmers University of Technology, Göteborg, Sweden.

Popper, R., Niemz, P., Eberle, G. (2004a) Equilibrium moisture content and swelling of the solid wood panels. Holz Roh Werkst. 62:209–217.

Popper, R., Niemz, P., Eberle, G. (2004b) Diffusion processes in multilayer solid wood panels. Holz Roh Werkst. 62:253–260.

Ranta-Maunus, A. (1990) Impact of mechano-sorptive creep to the long-term strength of timber. Holz Roh Werkst. 48:67–71.

Santaoja, K., Leino, T., Ranta-Maunus, A., Hanhijärvi, A. (1991) Mechano-sorptive structural analysis of wood by the ABAQUS finite element program. Research Notes 1276, Technical Research Center of Finland, Espoo.

Sell, J. Eigenschaften und Kenngrössen von Holzarten. Baufachverlag AG, Dietikon, 1997.

Siau, J.F. Wood: Influence of Moisture on Physical Properties. Department of Wood Science and Forest Products, Virginia Polytechnic Institute and State University, Blacksburg, USA, 1995.

Takemura, T. (1967) Plastic properties of wood in relation to the non equilibrium states of moisture content. Part II. Mokuzai Gakkaishi 13:77–81.

Tobisch, S. (2006) Methoden zur Beeinflussung ausgewählter

Eigenschaften von dreilagigen Massivholzplatten aus Nadelholz. PhD thesis, University of Hamburg, Germany.
Toratti, T. (1992) Creep of timber beams in a variable environment. PhD thesis, Helsinki University of Technology, Finland.
Vanek, M., Teischinger, A. (1989) Diffusionskoeffizienten und Diffusionswiderstandszahlen von verschiedenen Holzarten. Holzforsch. Holzverwert. 1:3–6.
Wadsö, L. (1994) Describing non-Fickian water-vapour sorption in wood. J. Mater. Sci. 29:2367–2372.

Received August 29, 2008. Accepted January 12, 2009.
Previously published online February 18, 2009.